Journal of the Nigerian Association of Mathematical Physics
Volume 57(**June – July** *2020 Issue*), **pp35 – 44**

MIXED FINITE ELEMENT METHODS FOR NUMERICAL WEATHER PREDICTION IN NIGERIA

[1]Jacob E., [2]Adeboye K.R.,[3]Victor A. O. and [4]Dahuwa D.

[1]Department of Mathematics, University of Abuja.
[2]Department of Mathematics, Federal University of Technology Minna.
[3]Department of Mathematics, Pan African University, Institute of Basic Science, Technology and Innovation, Kenya
[4]Department of Physics, Aminu Saleh CO E., Azare Bauchi State

Abstract

In this paper, the finite element methods, which can be thought of as the finite element extension of the C-grid staggered finite difference method is used to streamline the impulse of some particular class of the wave equations. Numerical estimation of the finite element method on weather data from the Federal Airports Authority of Nigeria (FAAN), Abuja was presented which shows a clear prediction through the developed model for future weather trends. Also a graphical and empirical representation of the numerical weather data from the model analysis was presented using MATLAB programming codes.

Keywords*:* finite element, prediction, mixed, staggered, spurious, difference.

1. Introduction

Mixed finite element method also known as the hybrid finite element method, is a type of finite element method in which extra independent variables are introduced as nodal variables during the discretization of a partial differential equation problem, they are generalization of staggered finite difference methods and are intended to address the same problem. Spurious pressure mode observed in the finite difference A-grid and are also observed in finite element methods when the same finite element method, difference finite spaces are selected for different variables. The vast range of available finite element spaces is both a blessing and a curse and many different combinations have been proposed, analyzed and used for large scale geological fluid dynamics applications, particularly in the ocean modeling community [1-2] whilst many other combinations have been used in engineering applications where different scales and modeling aspects are relevant.

The finite element methods, which can be thought of as the finite element extension of the C-grid staggered finite difference method is used to streamline the impulse of some particular class of the wave equations. This class is always referred to as compatible finite elements, mimetic finite elements, discrete differential forms or finite element exterior calculus. This family of mixed finite element methods is used in the numerical weather prediction as a generalization for the popular polygonal C-grid finite difference methods in this study. There are a few major advantages: the mixed finite elements do not require an orthogonal grid, and they allow a degree of flexibility that can be exploited to ensure an appropriate ratio between the velocity and pressure degrees of freedom so as to avoid spurious mode branches in the numerical dispersion relation. These methods preserve several properties of the C-grid method when applied to linear barotropic wave propagation, namely; (a) Energy conservation, (b) Mass conservation, (c) No spurious pressure modes, (d) Steady geostrophic modes on the f-plane. All of these finite element methods have an exact 2:1 ratio of velocity degrees of freedom to pressure degrees of freedom.

In this paper, we are discussing only a particular family of mixed finite element methods known as discrete differential forms or finite element exterior calculus. This finite element methods have the important property that differential operators such as grad and curl map form one finite element space; this embedding property lead to discrete versions of the div-curl and curl-grad identities of vector calculus. This properties of the C-grid finite difference method discussed in full generality on unstructured grids. And shown to be highly relevant and useful in geophysical fluid dynamics applications. This generalization of the C-grid method is very useful since it allows (i) the arbitrary grids, with no requirement of orthogonal grids without loss of consistency/convergence rate. (ii) extra flexibility in the choice of discretization to optimize the ration between global velocity degrees of freedom (DoFs) and global pressure DoFs to eliminate spurious mode branches and (iii) the option to increase the consistency/convergence order.

Mixed finite element methods were first identified in the 1970s and quickly became very popular amongst numerical analysts since the additional mathematical structure facilitated proofs of stability and convergence and provided powerful insight. This result were collected and unified in [3] and excellent book which has been out of print for a long time but a new addition has recently appeared [4]. This methods have become a standard tool for ground water modeling using Darcy's law [5]and have also become very popular for solving Maxwell's equations [6] where a mathematical structure based on differential forms was developed by[6], together with the term "discrete differential forms." This structured was enriched, extended and unified under the term " finite exterior calculus" by Douglas Arnold and collaborators [7], who used the framework to develop new stable.

Corresponding Author**:** Jacob E., Email: jacobemma001@gmail.com, Tel: +2348032259737

Recently, there have been further developments in the application of compatible finite element methods to the nonlinear shallow water equations on the sphere, an efficient software implementation of the mixed finite element spaces on the sphere provided. In this research we cover the general introduction to finite element computations, compatible finite element solutions for one-dimensional and three-dimensional wave equations, staggered outlook towards application of analytic solutions of n-dimensional wave equations and compressible dynamic cores.

Continuity Equation for the Finite Element Method

The governing equations for quasi-static motions in a homogenous incompressible fluid with a free surface (shallow atmospheric weather equation) can be written as

$$\frac{\partial \boldsymbol{v}}{\partial t} + qk \times v^* + \nabla(K + \Phi) \ = 0 \qquad (1)$$

$$\frac{\partial h}{\partial t} + \nabla \cdot v^* = 0 \qquad (2)$$

Here v is the horizontal velocity, t the time, $q \equiv (f + \zeta)/h$ the potential velocity, f the Coriolis parameter, $\zeta \equiv k \cdot \nabla \times v$ the relative velocity, h the depth of a fluid column above the bottom surface, k the vertical unit vector, $v^* \equiv hv$ the horizontal mass flux, ∇ the horizontal del operator, $K \equiv {v^2}/{2}$ the horizontal kinetic energy per unit mass, $\Phi \equiv g(h + h_s)$ the geo-potential at the free surface, g the gravitational acceleration and $h_s$the height of the bottom surface.

Multiplying (1) by $v^*$and using (2), we obtain the equation for the time change of kinetic energy,

$$\frac{\partial}{\partial t}(hk) + \nabla \cdot (v^* K) + v^* \cdot \nabla\Phi = 0 \qquad (3)$$

Multiplying (2) byΦ, on the other hand, we obtain the equation for time change of potential energy,

$$\frac{\partial}{\partial t}\left[\frac{1}{2}gh^2 + ghh_s\right] + \nabla \cdot (v^* \cdot \Phi) - v^* \cdot \nabla\Phi = 0 \qquad (4)$$

The sum of (3) and (4) yields conservation of total energy,

$$\overline{\frac{\partial}{\partial t}\left[h\left(K + \frac{1}{2}gh + gh_s\right)\right]} = 0 \qquad (5)$$

Where the over bar denotes the area mean over a periodic domain or a domain with no inflow or outflow through the boundaries.

Operating $k \cdot \nabla$ on (1), we obtain the vorticity equation that is equivalent to the form of the potential vorticity equation given by

$$\frac{\partial}{\partial t}(hq) + \nabla \cdot (v^* q) = 0 \qquad (6)$$

Subtracting (2) times q from (2.6), we obtain

$$\frac{\partial q}{\partial t} + v \cdot (\nabla q) = 0 \qquad (7)$$

That is the advective form of the potential vorticity equation. In the case of nondivergent mass flux, for which $\nabla \cdot v^* = 0$ (and $\frac{\partial h}{\partial t} = 0$), we can define a streamfucntion $\psi^*$for the mass flux by

$$v^* = k \times \nabla\psi^* \qquad (8)$$

Then, using Cartesian coordinates x and y, we can express (1.6) as

$$\frac{\partial}{\partial t}(hq) + J(\psi^*, q) = 0 \qquad (9)$$

Where J is the Jacobian defined by

$$J(a, b) \equiv \frac{\partial a}{\partial x}\frac{\partial b}{\partial y} - \frac{\partial a}{\partial y}\frac{\partial b}{\partial x} \qquad (10)$$

Multiplying (7) by $hq$and using (2), we obtain the potential entropy equation

$$\frac{\partial}{\partial t}\left(h\frac{1}{2}q^{2n}\right) + \nabla \cdot \left(v^* \frac{1}{2}q^2\right) = 0 \qquad (11)$$

That leads to conservation of potential entropy

$$\overline{\frac{\partial}{\partial t}\left(h\frac{1}{2}q^2\right)} = 0 \qquad (12)$$

One Dimensional Formulation

In this section we develop the compatible finite element method in the context of the one-dimensional scalar wave equation on the domain [0, L] with periodic boundary conditions,

$$h_{tt} - h_{xx} = 0, \ h(0, t) = h(L, t) \qquad (13)$$

Figure 1: Example finite element functions for a subdivision of the domain [0, 1] into 10 elements. Left: A function from the finite element space (CG1). Right: A function from the finite space (DG 0) (Majewski, 2002).

It is more relevant to issues arising in the shallow atmospheric weather equations, and beyond, to split this equation into two first order equations, in the form

$$u_t + h_x = 0, \qquad h_t + u_x = 0, \qquad h(0,t) = h(L,t), \qquad u(0,t) = u(L,t) \qquad (14)$$

We shall discretise (14) in space using compatible finite element methods

In general, the finite element method is based on two key ideas:

i) The approximation of the numerical solution by functions from some chosen finite element spaces, and

ii) The weak form

Finite element space (on a one-dimensional domain): we partition the interval [0, L] into $N_e$non-overlapping subintervals, which we call elements; the partition is called a mesh. We shall call the point shared by two neighboring elements a vertex. A finite element space is a collection of functions on [0, L] which are:

1. Polynomials of some specified maximum degree p when restricted to each element e, and
2. Have some specified degree of continuity (discontinuity, continuous, continuous derivative, etc.)

The most common options for continuity are continuous functions, in which case we name the finite element space CG(p) for give p, and discontinuous functions, in which case we name the finite space DG(p) (higher order continuity finite element spaces are more exotic, B-splines for example, and we shall not discuss them in this research). An example function from the CG 1 space and an example function from the DG 0 space are shown in Figure 1.We use the term finite element space since the collection of functions form a vector space (i.e. they may be added together and scaled by real numbers, and addition and scaling satisfy the required properties of a vector space). This makes finite element amenable to the tools of linear algebra. We also note that finite element spaces are finite dimensional. This makes them amenable calculation on a computer.

In a bid to Discretized (14), we restrict h and u to finite element spaces, let us say CG 1 for the purpose of this research (we will use the notation $u \in CG1$to mean that u is a function in the finite space. Clearly we do not obtain solutions of (2.14), since if $u \in CG1$ then$u_x \in DG0$. (The DG 0 was obtained in Figure 1 by taking the derivative of the CG 1 function.).Hence, we choose to find the best possible approximation to (14) by minimizing the magnitude of $u_t + h_x \; and \; h_t + u_x$whilst keeping u and h in CG 1. To do this, we need to choose a way of measuring the magnitude of functions (*i.e.*, a norm) of which the L^2 norm, given by

$$\|u\|_{L^2} = \sqrt{\int_0^L u^2 dx}, \qquad (15)$$

Is the most natural and computationally feasible. The finite element approximation becomes

$$\min_{u_t \in CG1} \frac{1}{2}\|u_t + h_x\|^2, \quad \min_{h_t \in CG1} \frac{1}{2}\|h_t + u_x\|^2, \qquad (16)$$

The standard calculus of variations approach to finding the minimiser $u_t$for the first Expression (17) follows from nothing if $u_t$is optimal, then infinitesimal changes in u_t do not change the value of $\|u_t + h_x\|^2$. This is expressed mathematically as

$$\lim_{\epsilon \to 0} \frac{\frac{1}{2}\|u_t + \epsilon\omega + h_x\|^2 - \frac{1}{2}\|u_t + h_x\|^2}{\epsilon} \qquad (17)$$

For any $\omega \in CG\ 1$ (we adopt the notation $\forall \omega \in CG\ 1$). We obtain

$$0 = \lim_{\epsilon \to 0} \frac{1}{2}\|u_t + \epsilon\omega + h_x\|^2 - \frac{1}{2}\|u_t + h_x\|^2,$$

$$= \frac{1}{2}\int_0^L (u_t + \epsilon\omega + h_x)^2\, dx - \frac{1}{2}\int_0^L (u_t + h_x)^2\, dx,$$

$$= \frac{1}{2}\int_0^L (u_t + h_x)^2\, dx + 2\epsilon\omega \int_0^L (u_t + h_x) dx - \frac{1}{2}\int_0^L (u_t + h_x)^2\, dx$$

$$= \int_0^L \omega(u_t + h_x) dx, \forall \omega \in CG\ 1 \qquad (18)$$

Similarly, the standard calculus of variations approach to finding the minimiser h_t for the second expression (17) follows from noting if $h_t$is optimal, then infinitesimal changes I h_t do not change the value of $\|h_t + u_x\|^2$. This is expressed mathematically as

$$\lim_{\epsilon \to 0} \frac{\frac{1}{2}\|h_t + \epsilon\emptyset + u_x\|^2 - \frac{1}{2}\|h_t + u_x\|^2}{\epsilon}, \qquad (19)$$

For any $\emptyset \in CG\ 1$ (we adopt the notation $\forall \emptyset \in CG\ 1$). We obtain

$$0 = \lim_{\epsilon \to 0} \frac{1}{2}\|h_t + \epsilon\emptyset + u_x\|^2 - \frac{1}{2}\|h_t + u_x\|^2,$$

$$= \frac{1}{2}\int_0^L (h_t + \epsilon\emptyset + u_x)^2\, dx - \frac{1}{2}\int_0^L (h_t + u_x)^2\, dx,$$

$$= \frac{1}{2}\int_0^L (h_t + u_x)^2\, dx + 2\epsilon\emptyset \int_0^L (h_t + u_x) dx - \frac{1}{2}\int_0^L (h_t + u_x)^2\, dx$$

$$= \int_0^L \emptyset(h_t + u_x) dx, \forall \emptyset \in CG\ 1 \qquad (20)$$

We refer to $\omega \; and \; \emptyset$ as *test functions*. Note that equations (20) and (21) can be directly obtained by multiplying Expression (17) by test functions $\omega \; and \; \emptyset$, and integrating over the domain; the minimisation process is only a theoretical tool to explain that it is the best possible approximation using the element space[9] Since these equations represent the error-minimising approximations of Expression (17) with $u \in CG\ 1, p \in CG\ 1$,we call them the *projections* of Expression (17) onto CG 1. In general, the projection of a function or an equation onto a finite element space is called *Galerkin projection*.

Equations (19 – 20) can be implemented efficiently on a computer by expanding $\omega, \emptyset, u \; and \; h$ in a basis over CG 1,

$$u(x) = \sum_{i=1}^{n} N_i(x)u_i\,, h(x) = \sum_{i=1}^{n} N_i(x)h_i\,, \omega(x) = \sum_{i=1}^{n} N_i(x)\omega_i\,, \emptyset(x)$$

$$\sum_{i=1}^{n} N_i(x)h_i\,, \omega(x) = \sum_{i=1}^{n} N_i(x)\emptyset_i \qquad (21)$$

With real valued basis coefficients $\omega_i, \emptyset_i, u_i \; and \; h_i$. These basis coefficients are still functions of time since we have not yet discretized in time yet. In general, in one dimension it is always possible to find a basis for CG(p) and DG(p) finite element spaces such that the basic functions $N_i$are non-zero in at most two (neighbouring) elements. Substitution of these basis expansions into Equations (19 – 21) gives

$$\omega^T(M\dot{u} + Dh) = 0, \qquad \emptyset^T\left(M\dot{h} + Du\right) = 0 \qquad (22)$$

Where *M* and *D* are matrices with entries given by

$$M_{ij} = \int_0^L N_i(x)N_j\,(x)dx, \qquad D_{ij} = \int_0^L N_i\,(x)\frac{\partial N_j}{\partial x}(x)dx, \qquad (23)$$

And $\boldsymbol{u, h, \omega}$*and*$\emptyset$are vectors of basis coefficients with $\boldsymbol{u} = (u_1, u_2, \dots, u_n)$etc. Equations (23)must hold for all test functions $\omega$and $\emptyset$, and therefore for arbitrary coefficient vectors ω and $\emptyset$. Therefore, we obtain the matrix-vector systems,

$$(M\dot{u} + Dh) = 0, \; \left(M\dot{h} + Du\right) = 0 \qquad (24)$$

Having chosen a basis where each basis function vanishes in all but two elements, the matrices *M* and *D* are extremely sparse and hence can be assembled efficiently Furthermore, the matrix *M*is well-conditioned and hence can be cheaply inverted using iterative methods

It remains to integrate Equations (24) using a discretization in time. A generalisation of this approach is used for all of the finite element methods that we describe in this research.

One key problem with Equations (21 – 22) is that of spurious modes. For example, if we use angular grid of N_e elements of the same size, if h is a CG1 ‘‘zigzag’’ function that alternates between 1 and -1 between each vertex, then $h_x$is a DG0 ‘‘flip-flop" function that takes the value Δx and $-\Delta x$ in alternate elements, where $\Delta x = Ne/L$. Multiplication by a CG1 test function ω and integrating then gives zero for arbitraryω. The easiest way to understand why is to choose ω to be a hat-shaped basis function that is equal to 1 at a single vertex, and zero at all other vertices. Then the integral of ω multiplied by h_x is a (scaled) average of $h_x$over two elements, which is equal to zero. Since all ω can be expanded in basis functions of this form, we obtain $D\omega$ in every case. This is a problem because our original zigzag function is very oscillatory, and so the approximation of the derivative should be large. In general, using the same finite element space for u and h leads to the existence of spurious modes which have very small numerical derivatives, despite being very oscillatory, and hence propagate very slowly. When nonlinear terms are introduced, these modes get coupled to the smooth part of the function, and grow rapidly, making the numerical scheme unusable.

In finite difference methods, this problem is avoided by using staggered grids, with different grid locations for u and h. In finite element methods, the analogous strategy is to choose different finite element spaces for u and h. This is referred to as a mixed finite element method.

We shall write $u \epsilon V_0, h \epsilon V_1$,and discuss different choices for V_0, and V_1. In particular, we shall choose $V_0 = CG\ 1 \; and \; V_1 = DG\ 0$,together with the higher-order extensions $V_0 = CG(p) \; and \; V_1 = DG(p-1)$, for some chosen p >1. The reason for doing this is that if $u \in V_1$,then $u_x \in V_1$:this is because u is continuous but can have jumps in the derivative, and differentiation reduces the degree of a polynomial by 1. We say that the finite element spaces V_0 and V_1 are compatible with the *x*-derivative. This choice means that $h_t + u_x \in V_1$and there is no approximation in writing that equation [1].

To write down our compatible finite element method we have one further issue to address, namely that $h \in V_1$is discontinuous, and so $h_x$is not globally defined. This is dealt with by integrating the $h_x$term by parts in the finite element approximation, i.e. from Equation (19) we have the resulting solution to be

$$\int_0^L \omega(u_t + h_x)dx = 0, \forall \omega \in CG\ 1$$

hen integrating by part we let $du = \omega dx \; and \; v = u_t + h_x$, therefore,

$u = \omega_x \; and \; dv = h$

$$\int vdu = uv - \int udv,$$

$$\int_0^L \omega(u_t + h_x)dx \; = \omega_x(u_t + h_x) - \int_0^L \omega_x h dx$$

By finite element approximation

$$\int_0^L \omega(u_t + h_x)dx = \int_0^L \omega u_t dx - \int_0^L \omega_x h dx$$

$$\int_0^L \omega(u_t + h_x)dx = \int_0^L (\omega u_t - \omega_x h)dx, \ \forall \omega \in V_0 \quad (25)$$

Similar solution exist by integrating the $u_t$term by parts in the finite element approximation for equation (21)

$$\int_0^L \emptyset(h_t + u_x)dx = 0, \forall \emptyset \in CG\ 1$$

Then integrating by part we let $du = \emptyset dx \ and \ v = h_t + u_x$, therefore,

$$u = \emptyset_x \ and \ dv = u$$

$$\int vdu = uv - \int udv,$$

$$\int_0^L \omega(h_t + u_x)dx = \emptyset_x(h_t + u_x) - \int_0^L \emptyset_x u dx$$

By finite element approximation

$$\int_0^L \emptyset(h_t + u_x)dx = \int_0^L \emptyset h_t dx - \int_0^L \emptyset_x u dx$$

$$\int_0^L \emptyset(h_t + u_x)dx = \int_0^L (\emptyset h_t - \emptyset_x u)dx, \ \forall \emptyset \in V_1 \quad (26)$$

There is no boundary term arising from integration by parts due to the periodic boundary conditions. Three out of the four terms in these two equations involve trivial projections that do nothing to the $u_t, h_t and\ u_x$ terms. This means that they introduce no further errors beyond approximating the initial conditions in the finite element spaces. The only term that we have to worry about is the discretized $h_x$term, where we would like to convince ourselves that there are no spurious modes[10]. This is done by showing that the following mathematical condition holds.

Inf-sup condition: The spaces V_0 and V_1satisfy the in f-sup condition if there exist a constant C>0, independent of the choice of mesh, such that

$$\sup_{\omega \in V_0, \omega \neq 0} \frac{\left|\int_0^L \omega_x h dx\right|}{\|\omega_x\|_{L^2}} \geq C\|h\|_{L^2}, \quad (27)$$

For all non-constant $h \in V_1$.

This prevents spurious modes because it says that for any non-constant *h*, there exist at least one *ω* such that the integral is reasonably large in magnitude compared to the size of $\omega_x \ and \ h$. In general, proving the inf-sup condition for mixed finite element methods is a fairly technical business. However, for our compatible finite element discretization, it is completely straightforward.

Inf-sup condition for compatible finite element: let $V_0$and V_1be chosen such that if $h \in V_1$is non-constant then we can find $\omega \in V_0$such that $\omega_x = h$. Then the inf-sup condition is satisfied, with C=1.

For any non-constant *h*, take ω'such that $\omega'_x = h$(which is possible by the condition above). Then

$$\sup_{\omega \in V_0} \frac{\left|\int_0^L \omega_x h dx\right|}{\|\omega_x\|_{L^2}} \geq \frac{\left|\int_0^L \omega'_x h dx\right|}{\|\omega'_x\|_{L^2}} = \frac{\|h\|^2_{L^2}}{\|h\|_{L^2}} = \|h\|_{L^2} \quad (28)$$

The assumption of the above condition is true whenever $V_0 = CG(p), V_1 = DG(p-1)$. This means that our compatible finite element methods will be free from spurious modes.

Discrete Helmholtz Decomposition for $P1_{DG} - P2$

In this section we show that the velocity – pressure space ($P1_{DG} - P2$) finite element discretisation has a discrete Helmholtz decomposition for $P1_{DG} - P2$ [10].

Embedding Conditions: let V be the chosen vector space of finite element velocity fields (in the case of $\mathbf{P1_{DG} - P2}$, V is the space$\mathbf{P1_{DG}}$**(Velocity Space)** of velocity fields u^δthat are linear in each triangular element, with no continuity constraints across element boundaries), and let H be the chosen vector space of finite element pressure fields in the case of $\mathbf{P1_{DG} - P2,}$ H is the space **P2 (Pressure Space)** of pressure fields h^δthat are quadratic in each triangular element and are constrained to be continuous across element boundaries.

1. The operator ∇ defined by the pointwise gradient
   $q^\delta(x) = \nabla h^\delta(x)$
   maps from H into V
2. The skew operator ⊥ defined by the pointwise formula
   $q^\delta(x) = (u^\delta(x))^\perp = (-u^\delta{}_2 u^\delta{}_1)$
   maps from V into itself

These are the only conditions that we use in this research and hence any properties extend to any other finite element pair that satisfies these conditions ($Pn_{DG} - P(n+1)$ with any n>1, for example).

Next we note that any two pressure fields $\emptyset^\delta, \psi^\delta$ in the pressure space P2 are orthogonal in the L^2 inner product,

$$\langle \nabla\psi^\delta, \nabla^\perp\emptyset^\delta\rangle_{L^2} = \int_\Omega \nabla\psi^\delta \cdot \nabla^\perp\emptyset^\delta dV = 0$$

Where Ω is the solution domain which is either the sphere, or periodic boundary conditions? Hence, any velocity field $\boldsymbol{u^\delta}$ in $P1_{DG}$ can be written uniquely in an orthogonal decomposition

$$\boldsymbol{u^\delta} = \overline{\boldsymbol{u}}^{\boldsymbol{\delta}} + \nabla\emptyset^\delta + \nabla^\perp\psi^\delta + \widehat{\boldsymbol{u}}^{\boldsymbol{\delta}}$$

Where $\overline{\boldsymbol{u}}^{\boldsymbol{\delta}}$ is independent of space, where $\emptyset^\delta and\ \psi^\delta$ are both in the space $\overline{P2}$, which consists of P2 functions with mean zero, *i.e.*

$$\int_\Omega \emptyset^\delta dV = \int_\Omega \psi^\delta dV = 0,$$

And where $\widehat{\boldsymbol{u}}^{\boldsymbol{\delta}}$ is orthogonal to the gradient or skew-gradient of any $\overline{P2}$ function α^δ, i.e.

$$\int_\Omega \widehat{\boldsymbol{u}}^{\boldsymbol{\delta}} \cdot \nabla\alpha^\delta dV = \int_\Omega \widehat{\boldsymbol{u}}^{\boldsymbol{\delta}} \cdot \nabla\alpha^\delta dV = 0.$$

Furthermore, if any such $\widehat{\boldsymbol{u}}^{\boldsymbol{\delta}}$ satisfies

$$\int_\Omega \left|\widehat{\boldsymbol{u}}^{\boldsymbol{\delta}}\right|^2 dV = 0$$

The $\widehat{\boldsymbol{u}}^{\boldsymbol{\delta}} = \mathbf{0}$, since $\widehat{\boldsymbol{u}}^{\boldsymbol{\delta}}$ is obtained from orthogonal completion.

This is identical to the Helmholtz decomposition for arbitrary continuous velocity fields in which any velocity field $\boldsymbol{u}$ can be written as a constant plus a gradient of a potential plus skew gradient of a stream function, except for the extra component $\hat{u}$. This extra component gives rise to the spurious inertial oscillations in the $P1_{DG}$ – P2 finite element discretisation. It is possible to describe a reduced velocity space, which we call H(P2), consisting of velocity fields which can be written as

$$\boldsymbol{v^\delta} = \overline{\boldsymbol{v}}^{\boldsymbol{\delta}} + \nabla\emptyset^\delta + \nabla^\perp\psi^\delta,$$

Where $\overline{\boldsymbol{v}}^{\boldsymbol{\delta}}$ is independent of space, where $\emptyset^\delta and\ \psi^\delta$ are both in the space $\overline{P2}$, i.e. we have removed the spurious velocity component. It is possible to project a $P1_{DG}$ velocity field $\boldsymbol{u^\delta}$ into H (P2), by first computing the mean component,

$$\overline{\boldsymbol{u}}^{\boldsymbol{\delta}} = \frac{\int_{\boldsymbol{\Omega}} \boldsymbol{u^\delta} dV}{\int_{\boldsymbol{\Omega}} dV},$$

And then extracting the velocity potential and stream function by solving

$$\int_\Omega \nabla\alpha^\delta \cdot \nabla\emptyset^\delta dV = \int_\Omega \nabla\alpha^\delta \cdot u^\delta dV,$$

and

$$\int_\Omega \nabla\alpha^\delta \cdot \nabla\emptyset^\delta dV = \int_\Omega \nabla^\perp\alpha^\delta \cdot u^\delta dV,$$

For all $\overline{P2}$ function α^δ. This amounts to solving elliptic problems for $\emptyset^\delta and\ \psi^\delta$. Then, the projection of u^δ into H(P2) is given by $\overline{\boldsymbol{u}}^{\boldsymbol{\delta}} + \nabla\emptyset^\delta + \nabla^\perp\psi^\delta$.

Discrete Wave Propagation on *f*-plane

In this section we describe all of the numerical solutions obtained from $P1_{DG}$ – P2 applied to the *f*-plane. The $P1_{DG}$ – P2 spatial discretisation of the rotating shallow-atmospheric weather equations is

$$\frac{d}{dt}\int_\Omega \omega^\delta \cdot u^\delta\, dV + \int_\Omega f\omega^\delta \cdot \left(u^\delta\right)^\perp dV = -c^2 \int_\Omega \omega^\delta \cdot \nabla\eta^\delta\, dV, \qquad (28)$$

$$\frac{d}{dt}\int_\Omega \emptyset^\delta\eta^\delta\, dV = \int_\Omega \nabla\emptyset^\delta \cdot u^\delta\, dV, \ldots$$

Where the velocity u^δ is in $P1_{DG}$, the layer depth $h^\delta = H(1+\eta^\delta)$ is in P2, for all test functions ω^δ in $P1_{DG}$ and $\emptyset^\delta$ in P2, and where $c^2 = gH$ the non-rotating wave propagation speed is, g is the acceleration due to gravity, H is the mean layer depth and f is the Coriolis parameter[1].

On the f-plane, f is a constant, and so we may take it outside the Coriolis integral. Applying the discrete Helmholtz decomposition to the velocity u^δ and the velocity test functions ω^δ, i.e.,

$$u^\delta = \overline{\boldsymbol{u}}^{\boldsymbol{\delta}} + \nabla\emptyset^\delta + \nabla^\perp\psi^\delta + \hat{u}, \qquad \omega^\delta = \overline{\boldsymbol{\omega}}^{\boldsymbol{\delta}} + \nabla\alpha^\delta + \nabla^\perp\beta^\delta + \hat{\omega},$$

Equation (1-2) become (after removing products of orthogonal quantities)

$$\frac{d}{dt}\langle\nabla\alpha^\delta, \nabla\emptyset^\delta\rangle - f\langle\nabla\alpha^\delta, \nabla\psi^\delta\rangle + c^2\langle\nabla\alpha^\delta, \nabla\eta^\delta\rangle = 0,$$

$$\frac{d}{dt}\langle\nabla\alpha^\delta, \nabla\psi^\delta\rangle + f\langle\nabla\alpha^\delta, \nabla\emptyset^\delta\rangle = 0,$$

$$\frac{d}{dt}\langle \alpha^{\delta}, \eta^{\delta}\rangle - \langle \nabla\alpha^{\delta}, \nabla\emptyset^{\delta}\rangle = 0 \quad (29)$$

$$\frac{d}{dt}\langle \bar{\boldsymbol{\omega}}, \bar{\boldsymbol{u}}\rangle + f\langle \bar{\boldsymbol{\omega}}, \bar{\boldsymbol{u}}\rangle = 0,$$

$$\frac{d}{dt}\langle \hat{\boldsymbol{\omega}}, \hat{\boldsymbol{u}}\rangle + f\langle \hat{\boldsymbol{\omega}}, \hat{\boldsymbol{u}}^{\perp}\rangle = 0,$$

These solutions exhibit four types of orthogonal modes: geostrophic balance, inertia gravity waves, the physical inertial oscillation, and spurious inertial oscillations due to the presence of $\widehat{\boldsymbol{U}}$. We shall now describe these modes one by one.

Geostrophic Balance: For the continuous equations before discretisation, geostrophically balanced modes are obtained from non-zero steady solutions of the equations. The P1$_{DG}$-P2 discretisation solutions which satisfy the geostrophic balance relation are also exactly steady. To see this within the framework of this research, assume a steady state, then equations (3-7) become

$$-f\langle \nabla\alpha^{\delta}, \nabla\psi^{\delta}\rangle + c^2\langle \nabla\alpha^{\delta}, \nabla\eta^{\delta}\rangle = 0 \quad (30)$$

At the next order we obtain

$$\frac{d}{dt}\langle \nabla\alpha^{\delta}, \nabla\phi^{\delta}{}_{ag}\rangle - f_0\,\langle \nabla\alpha^{\delta}, \nabla\psi^{\delta}{}_{ag}\rangle - \langle \beta y\nabla\alpha^{\delta}, \nabla\psi^{\delta}{}_{g}\rangle + gH\,\langle \nabla\alpha^{\delta}, \nabla\eta^{\delta}{}_{ag}\rangle = 0 \quad (31)$$

$$\frac{d}{dt}\langle \nabla\alpha^{\delta}, \nabla\psi^{\delta}{}_{g}\rangle + f_0\,\langle \nabla\alpha^{\delta}, \nabla\phi^{\delta}{}_{ag}\rangle + \langle \beta y\nabla\alpha^{\delta}, \nabla^{\perp}\psi^{\delta}{}_{g}\rangle = 0 \quad (32)$$

$$\frac{d}{dt}\langle \alpha^{\delta}, \eta^{\delta}{}_{g}\rangle - \langle \nabla\alpha^{\delta}, \nabla\phi^{\delta}{}_{ag}\rangle = 0, \quad (33)$$

$$f_0\langle \bar{\omega}, \bar{u}^{\perp}{}_{ag}\rangle + \langle \bar{\omega}\beta y, -\nabla\psi^{\delta}{}_{g}\rangle = 0 \quad (34)$$

$$f_0\langle \hat{\omega}, \hat{u}^{\perp}{}_{ag}\rangle + \langle \hat{\omega}\beta y, -\nabla\psi^{\delta}{}_{g}\rangle = 0 \quad (35)$$

Noticed that the spurious velocity modes do not appear at this order in the physical mode equations (31-33), and that equation (35) states that the geotropic spurious velocity modes are slated to the geotropic stream function. Substituting equations (30) and (33) into (32) gives

$$\frac{d}{dt}\left(\langle \nabla\alpha^{\delta}, \nabla\psi^{\delta}{}_{g}\rangle + \frac{f^2{}_0}{gH}\langle \alpha^{\delta}, \psi^{\delta}{}_{g}\rangle\right) + \langle \beta y\nabla\alpha^{\delta}, \nabla^{\perp}\psi^{\delta}{}_{g}\rangle = 0 \quad (36)$$

The second term in equation (35) may be written as

$$\langle \beta y\nabla\alpha^{\delta}, \nabla^{\perp}\psi^{\delta}{}_{g}\rangle = \langle \nabla\left(\beta y\alpha^{\delta}\right) - \beta\alpha^{\delta}(0,1), \nabla^{\perp}\psi^{\delta}{}_{g}\rangle = -\beta\,\langle \alpha^{\delta}, \frac{\partial}{\partial x}\psi^{\delta}{}_{g}\rangle \quad (37)$$

And we obtain the usual continuous finite element approximation to the Rossby wave equation using P2 elements

$$\frac{d}{dt}\left(\langle \nabla\alpha^{\delta}, \nabla\psi^{\delta}{}_{g}\rangle + \frac{f^2{}_0}{gH}\langle \alpha^{\delta}, \psi^{\delta}{}_{g}\rangle\right) - \beta\,\langle \alpha^{\delta}, \frac{\partial}{\partial x}\psi^{\delta}{}_{g}\rangle = 0 \quad (38)$$

Since *P2* elements are used, the approximation to the Rossby wave equation is third-order accurate. We again expect that the phase velocity is more independent of mesh orientation than other second-order methods. Since the stream function ψ^{δ} and the height variable η^{δ} are both from the *P2* space and hence have the same numbers of degrees of freedom, there are exactly twice as many inertia-gravity wave modes .

We also note that if the reduced space *H (P2)-P2* is used instead of P1$_{DG}$*-P2* we obtain the same equations but with vanishing spurious modes.

Finite Elements for Geophysical Fluid Dynamics

In this section we describe how mixed finite elements can be used to build flexible discretisations on pseudo-uniform grids. We concentrate on the rotating shallow-atmospheric weather equations which are regarded in the numerical weather prediction community as being a simplified model that contains many of the issues arising in the horizontal discretisation for dynamical core. Since in this research we are concerned with wave propagation properties, we restrict attention to the linearised equations on the *f*-plane, and β-plane or the sphere. First, we introduce the mixed finite element formulation applied to the linear rotating shallow-atmospheric weather equations, then we discuss various properties of the formulation that are a requirement for numerical weather prediction applications, namely global energy and local mass conservation, absence of spurious pressure modes and steady geotropic states [8]. These properties all rely on exact sequence properties i.e. div-curl relations.

Spatial Discretisation of the Linear Rotating Shallow-atmospheric Weather Equations

In this research we consider the discretisation of the linear rotating shallow-atmospheric weather equations on a two dimensional surface Ω that is embedded in three dimensions (which we restrict to be compact with no boundaries, e.g. the sphere or double periodic $x-y$ plane):

$$u_t + fu^{\perp} + c^2\nabla\eta = 0, \qquad \eta_t + \nabla\cdot u = 0, \qquad u\cdot n = 0 \ \ on\ \partial\Omega \quad (39)$$

Where $\boldsymbol{u} = (u, v)$ is horizontal velocity, $\boldsymbol{u}^{\perp} = k\times u, f$ is the Coriolis parameter, $c^2 = gH, g$ is the gravitational acceleration, H is the mean layer thickness, $h = H(1+\eta)$ is the layer thickness, $\boldsymbol{k}$ is the normal to the surface Ω, and ∇ and $\nabla\cdot$ are appropriate invariant gradient and divergence operators defined on the surface. We form the finite element approximation by multiplying by time-independent test functions $\boldsymbol{\omega}$ and ϕ, integrating over the domain, integrating the pressure gradient term $c^2\nabla\eta$ by parts in the momentum equation, and finally restricting the velocity trial and test functions $\boldsymbol{u}$ and $\boldsymbol{\omega}$ to a finite element subspace $S\subset H(div)$ (where $H(div)$ is the space of square integrable velocity fields whose divergence is also square integrable), and the elevation trial and test functions η and α to the finite element subspace $V\subset L^2$ (where $\square^2$ is the space of square integrable functions):

$$\frac{d}{dt}\int_{\Omega} \boldsymbol{\omega}^h \cdot \boldsymbol{u}^h dV + \int_{\Omega} f\boldsymbol{\omega}^h \cdot (\boldsymbol{u}^h)^{\perp} dV - c^2 \int_{\Omega} \nabla \cdot \boldsymbol{\omega}^h \eta^h \, dV = 0, \forall \boldsymbol{\omega}^h \in S \qquad (40)$$

$$\frac{d}{dt}\int_{\Omega} \alpha^h \eta^h dV + \int_{\Omega} \alpha^h \nabla \cdot \boldsymbol{u}^h dV = 0, \qquad \forall \alpha^h \in V, \qquad (41)$$

After discretisation in time, these equations are solved in practice by introducing basis expansions for $\boldsymbol{\omega}^h, \boldsymbol{u}^h, \eta^h, and\ \alpha^h$and solving the resulting matrix-vector systems for the basis coefficients [4].
In this framework we restrict the choice of finite element spaces *S* and *V* so that
$\boldsymbol{u}^h \in S \Longrightarrow \nabla \cdot u^h \in V$.
The divergence should map from S onto V, so that for all functions $\phi^h \in V$ there exist a velocity field $\boldsymbol{u}^h \in S$with $\nabla \cdot \boldsymbol{u}^h = \phi^h$. Such spaces are known as ''div-conforming''. Furthermore we require that there exists a ''steam function'' space $E \subset H^1$such that
$\psi^h \in E \Longrightarrow \boldsymbol{k} \times \nabla \psi^h \in S$,
Where the $\boldsymbol{k} \times \nabla$operator (the curl, which we shall write as $\nabla^{\perp}$)maps onto the kernel of $\nabla \cdot$ in S. A consequence of these properties is that functions in *E* are continuous, vector fields in *S* only have continuous normal components and functions in *V* are discontinuous [3]

Energy Conservation

Global energy conservation for the linearised equations is a requirement of numerical weather prediction models for various reasons, in particular because it helps to prevent numerical sources of unbalanced fast waves. It is also a precursor to energy-conserving discretisation of the nonlinear equations using the vector-invariant formulation. For the mixed finite element method, global energy conservation is an immediate consequence of the Galerkin finite element formulation. The conserved energy of equation (4.) is

$$H = \frac{1}{2}\int_{\Omega} |\boldsymbol{u}|^2 + c^2\eta^2 dV.$$

Substituting the solution $\boldsymbol{u}^h and\ \eta^h$to equation (4 – 5) and taking the time derivative gives

$$\frac{d}{dt}H = \int_{\Omega} \boldsymbol{u}^h \cdot \boldsymbol{u}^h + c^2\eta^2 \cdot \eta^2 dV.$$

Choosing $\boldsymbol{\omega}^h = \boldsymbol{u}^h$ and α^h and h^h to equations (1.40 – 1.41) then gives

$$\frac{d}{dt}H = \int_{\Omega} \boldsymbol{u}^h \cdot \boldsymbol{u}^h + c^2\eta^h \cdot \eta^h dV$$

$$\frac{d}{dt}H = \int_{\Omega} -f \underbrace{\boldsymbol{u}^h \cdot (\boldsymbol{u}^h)^{\perp}}_{=0} + \underbrace{c^2\nabla \cdot \boldsymbol{u}^h\eta^h - c^2\eta^h\nabla \cdot \boldsymbol{u}^h}_{=0} dV = 0.$$

Local Mass Conservation

Local mass conservation is a requirement for numerical weather prediction models since it prevents spurious sources and sinks mass. For the nonlinear density equation, this can be achieved using a finite volume or discontinuous Galerkin method. For mixed finite element methods of the type used in this research applied to the linear equations, consistency and discontinuity of functions in *V* require that element indicator functions (i.e., functions that are equal to 1 in one element and 0 in the other) are contained in *V*. Selecting the element indicator function for element *e* as the test function α^hin equation (41) gives

$$\frac{d}{dt}\int_{e} \eta^h dV + \int_{\partial e} \boldsymbol{u}^h \cdot \boldsymbol{n} dS = 0,$$

Where ∂eis the boundary of element e. Since $\boldsymbol{u}^h$has continuous normal components on element boundaries, this means that flux of η^h is continuous and hence η^h is locally conserved [2]

Main Results

Station: Abuja, NG Elev: 343.1ft. Lat: 09.15°N Lon: 07.00°E

STATION NUMBER	STATION NAME	ELEV	LAT	LONG	DATE/MONTH	RelHum	TMAX	TMIN	RAINFALL	SUNSHINE HRS	WIND SPEED	WIND DIRECTION
65125	**Abuja**	**343.1**	**09.15' N**	**07.00' E**	201801	44	34.5	18.3	0	7.3	3.9	E
65125	**Abuja**	**343.1**	**09.15' N**	**07.00' E**	201802	49	**36.4**	**24.2**	**0**	**9.5**	**4.7**	E
65125	**Abuja**	**343.1**	**09.15' N**	**07.00' E**	201803	61	**36.7**	**24**	**0**	**9.2**	**4.5**	NE
65125	**Abuja**	**343.1**	**09.15' N**	**07.00' E**	201804	61	**37.6**	**25**	**4.2**	**8.5**	**6**	E
65125	**Abuja**	**343.1**	**09.15' N**	**07.00' E**	201805	74	**36.8**	**26**	**79.2**	**8.4**	**5.2**	W
65125	**Abuja**	**343.1**	**09.15' N**	**07.00' E**	201806	80	**32.2**	**22.3**	**167.2**	**6.5**	**5.0**	SW
65125	**Abuja**	**343.1**	**09.15' N**	**07.00' E**	201807	85	**29.7**	**21.3**	**214.8**	**5.5**	**4.3**	SW
65125	**Abuja**	**343.1**	**09.15' N**	**07.00' E**	201808	88	**29.7**	**21.5**	**278.3**	**4.3**	**4.9**	SW
65125	**Abuja**	**343.1**	**09.15' N**	**07.00' E**	201809	84	**30.5**	**23.2**	**158.4**	**4.2**	**4.9**	E
65125	**Abuja**	**343.1**	**09.15' N**	**07.00' E**	201810	79	**32**	**22.8**	**138.2**	**4.8**	**4.6**	SW
65125	**Abuja**	**343.1**	**09.15' N**	**07.00' E**	201811	65	**34**	**24**	125.5	**9.7**	**4**	E
65125	**Abuja**	**343.1**	**09.15' N**	**07.00' E**	201812	38	**35.5**	**18.3**	**130.0**	**9.8**	**4.2**	NE

Source: FAAN

Table 1. Compatible FEM Weather Prediction (2018)

Below are the various vector plots showing the attenuation of the monthly temperature, relative humidity, rainfall and wind speed of 2018

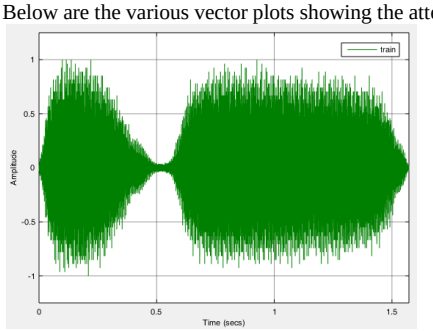

Figure 1: An animated graph showing radar view of the telephonic grid formation along the coastal axis from the atmospheric weather prediction model in the Federal Capital Territory, Abuja, Nigeria on 13/07/2018. Image was gotten using MATLABR2018a.

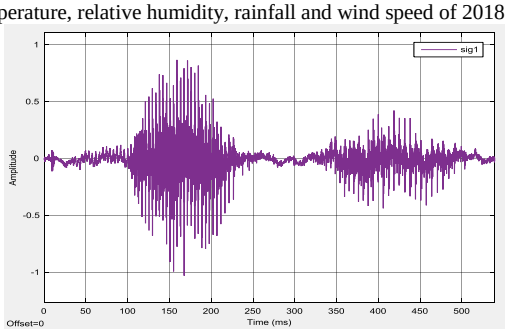

Figure 2: An animated graph showing pixel view of the grid formation along the coastal axis from the weather prediction model in the Federal Capital Territory, Abuja, Nigeria on 13/007/2018. Image was gotten using MATLAB R2018a

DATE AND TEMPERATURE ANALYSIS

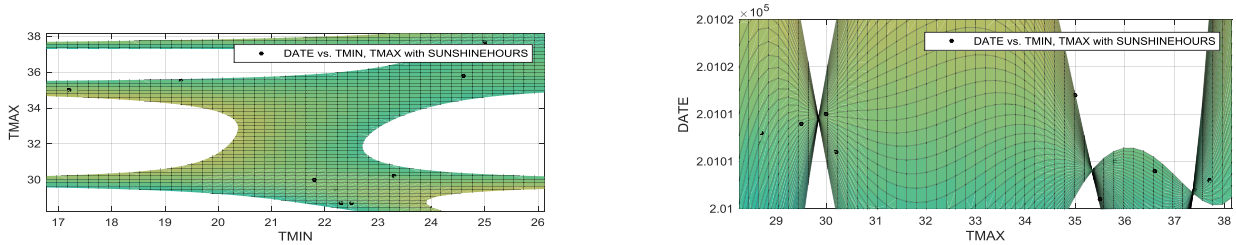

Figure 3: The 3D image shows the temperature will be high from around March to beginning of the last quarter of the year and that will definitely affect the relative humidity and hence increase evaporation, therefore, rainfall with be high and short. Image was gotten using MATLAB R2018a.

DATE AND MAXIMUM TEMPERATURE

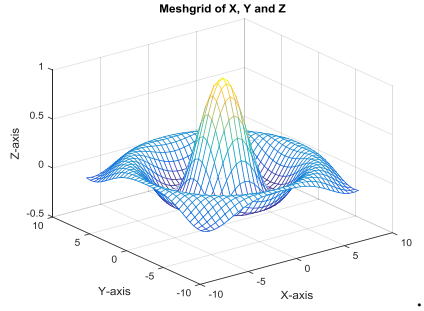

Figure 4: Animated image showing mesh grid attenuation of rainfall (Z) around periods of high (Y) and low (X) temperature. Image was gotten using MATLAB R2018a.

Conclusion

In Conclusion the weather prediction for a station (i.e. Abuja, Nigeria) was flexibly obtained accurately prior to the use of previously determined or forecasted data using a mixed finite element extension of a C-grid staggered finite difference method. The finite element methods, which can be thought of as the finite element extension of the C-grid staggered finite difference method is used to streamline the impulse of some particular class of the wave equations. Numerical estimation of the finite element method on weather data from the Federal Airports Authority of Nigeria (FAAN), Abuja was presented which shows a clear prediction through the developed model for future weather trends. Also a graphical and empirical representation of the numerical weather data from the model analysis was presented using MATLAB programming codes.

Conflicts of Interest

The authors declare that there is no conflict of interest

REFERENCES

[1] Cotter, C. J., Ham, D. A., Pain, C. C., (2009). A Mixed Discontinuous/Continuous Finite Element Pair for Shallow-Water Ocean Modelling. Ocean Modelling 26, 86-90.

[2] Cotter, C., Ham, D., (2011). Numerical Wave Propagation for the Triangular P1DG-P2 Finite Element Pair. Journal of Computational Physics 230 (8), 2806 – 2820.

[3] Comblen, R., Lambrechts, J., Remacle, J.-F., Legat, V., (2010). Practical Evaluation of Five Partly Discontinuous Finite Element Pairs for the Non-Conservative Shallow Atmospheric Equations. International Journal for Numerical Methods in Fluids 63 (6), 701 – 724.

[4] Brezzi, F., Fortin, M., (1991). Mixed and Hybrid Finite Element Methods. Springer-Verlag New York, Inc.
[5] Boffi, D., Brezzi, F., Fortin, M., (2013). Mixed Finite Element Methods and Applications. Springer
[6] Allen, M. B., Ewing, R. E., Koebbe, J., (1985). Mixed Finite Element Methods for Computing Ground Atmospheric Weather Velocities. Numerical Methods For Partial Differential Equations 1 (3), 195 – 207.
[7] Bossavit, A., (1988). Whitney forms: A Class of Finite Elements for Three-Dimensional Computations in Electromagnetism. IEE Proceedings A (Physical Science, Measurement and Instrumentation, Management and Education, Reviews) 135 (8), 493-500.
[8] Arnold, D., Falk, R., Winther, R., (2010). Finite Element Exterior Calculus: from Hodge Theory to Numerical Stability. Bull. Amer. Math. Soc.(NS) 47 (2), 281-354.
[9] Arakawa, A. and Lamb (1976). Computational Design of the UCLA General Circulation Model. In Methods in Computational Physics. Academic Press, New York.
[10] Cotter, C., Shipton, J., (2012). Mixed Finite Elements for Numerical Weather Prediction. Journal of Computational Physics 231 (21), 7076-7091.